Published in Water Resources Research 45, issue 3, 1–10, 2009
which should be used for any reference to this work

Behavior of a shallow water table under periodic flow conditions

Nick Cartwright,[1] Peter Nielsen,[2] and Pierre Perrochet[3]

[1] A new laboratory data set on the behavior of a shallow water table in a sand column aquifer subject to simple harmonic periodic forcing at its base is presented and discussed. The data are analyzed using the dynamic effective porosity, which is defined as the ratio of the rate of change in total moisture to the rate of change in water table elevation; thus, a reduction in this parameter means that the extent of moisture exchange has been reduced relative to a given water table fluctuation. The data show a clear decrease in the dynamic effective porosity with increasing proximity of the water table to the sand surface, which is consistent with previous research under a steadily rising or falling shallow water table. The observed reduction in moisture exchange due to shallowness of the water table has implications for periodic flow scenarios such as the propagation of water table waves in coastal and beach groundwater systems. That is, as moisture exchange is reduced, less work is being done by the flow, and thus, energy dissipation rates for shallow water tables will be reduced relative to the case of a deeper water table. At present no account of the influence of water table shallowness has been included in theories describing water table wave dispersion. The present experiments, in conjunction with the dynamic effective porosity concept, provide a framework in which this gap in knowledge can be further investigated. Additional experiments were designed such that the free surface transgressed the sand surface for part of the oscillation period to investigate the influence of meniscus formation and deformation at the sand surface on periodic flow dynamics. The observed behavior is consistent with previous observations of steady infiltration above shallow water tables, namely, a rapid drop (rise) in pore pressure with the onset of meniscus formation (deformation). A simple ''wetting and drying'' model is derived, accounting for the variation in effective porosity caused by the free surface transgressing the sand surface, which is shown to accurately capture the observed behavior. A finite element solution of the Richards equation in which the transient upper boundary condition is easily mimicked by means of a surface element with special storage features also shows excellent agreement with the observed data.

1. Introduction

[2] The significance of the influence of the capillary fringe on water table dynamics has been well documented in the literature [e.g., *Parlange and Brutsaert*, 1987; *Barry et al.*, 1996; *Li et al.*, 1997; *Lehmann et al.*, 1998; *Nielsen and Perrochet*, 2000; *Stauffer and Kinzelbach*, 2001; *Cartwright et al.*, 2005]. In all of these studies however, the distance from the water table to the surface of the porous medium was either assumed to be (theoretical work) or was set to be (experimental work) large enough such that there was no truncation of the capillary fringe.

[3] The influence of a shallow water table on moisture exchange has also been recognized in the literature. *Childs* [1969] described how the apparent specific yield, the volume of water released per unit area per unit drop in water table elevation, decreases significantly as the initial water table approaches the surface (as cited by *Duke* [1972]). *Duke* [1972] quantified this reduction in apparent specific yield as a function of the moisture distribution and proximity to the surface where the moisture distribution was described using the empirical *Brooks and Corey* [1964] power function.

[4] *Nachabe* [2002] later showed that *Duke*'s [1972] result was only valid for small changes in the water table elevation and went on to derive an analytical expression for a transient specific yield that is valid for any change in water table elevation. *Fayer and Hillel* [1986] and *Nachabe et al.* [2004] conducted research under conditions with a shallow rising water table responding to rainfall and also found a reduction in the transient specific yield due to proximity of the soil surface. All the transient specific yield models outlined above were derived for cases of a falling [*Duke*, 1972; *Nachabe*, 2002] or rising [*Fayer and Hillel*, 1986; *Nachabe et al.*, 2004] water table only.

[5] For periodic flow systems the use of the term effective porosity as opposed to transient specific yield is

[1]Griffith School of Engineering, Griffith University, Southport, Queensland, Australia.
[2]Division of Civil Engineering, University of Queensland, Brisbane, Queensland, Australia.
[3]Centre of Hydrogeology, University of Neuchâtel, Neuchâtel, Switzerland.

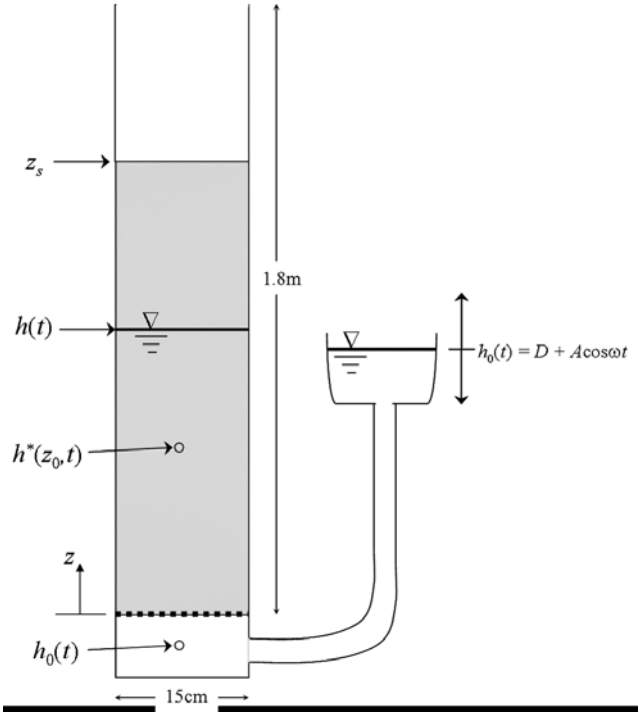

Figure 1. Schematic of the experimental sand column.

generally considered to be more appropriate. *Nielsen and Perrochet* [2000] introduced the concept of a dynamic effective porosity n_ω to describe the relationship between periodic fluctuations in the equivalent saturated height of total moisture h_{tot} (= h + h_c with h_c the equivalent saturated height of the unsaturated zone) and those in the water table h,

$$n\frac{\mathrm{d}h_{tot}}{\mathrm{d}t} = n_\omega\frac{\mathrm{d}h}{\mathrm{d}t} \tag{1}$$

where n is the usual effective (or drainable) porosity (=$\theta_s - \theta_r$, where θ_s is the saturated moisture content and θ_r is the residual moisture content [e.g., *Bear*, 1972] and the subscript ω was proposed by *Cartwright et al.* [2005] who extended the work of *Nielsen and Turner* [2000] and demonstrated the strong dependence of n_ω on oscillation frequency ω.

[6] The dynamic effective porosity (n_ω) can therefore be thought of as a dynamic analogy to the transient specific yield discussed in previous studies as it represents the rate of change in moisture ($\mathrm{d}h_{tot}/\mathrm{d}t$) relative to the rate of change in the water table ($\mathrm{d}h/\mathrm{d}t$),

$$\frac{n_\omega}{n} = \frac{\mathrm{d}h_{tot}}{\mathrm{d}t}\Big/\frac{\mathrm{d}h}{\mathrm{d}t} \tag{2}$$

The sand column data of *Nielsen and Perrochet* [2000] demonstrated that fluctuations in the total moisture were both damped and lagged those in the water table. These two observations can be conveniently accounted for by making n_ω complex in nature such that the damping is accounted for by its magnitude ($|n_\omega|/n$) and the lag by its argument ($Arg\{n_\omega/n\}$).

[7] In the development of the dynamic (complex) effective porosity concept to date [*Nielsen and Perrochet*, 2000; *Nielsen and Turner*, 2000; *Cartwright et al.*, 2005], the influence of the proximity of the sand surface was not investigated. Water table shallowness in periodic flow systems was the focus of a recent discussion by *Hilberts and Troch* [2006] who suggested that the proximity of the water table to the surface had influenced the results of sand column experiments by *Cartwright et al.* [2005]. *Cartwright et al.* [2006] agreed that the proximity of the surface may have influenced the upper parts of the moisture distribution but demonstrated that any such effect had not influenced the water table dynamics for the range of variables examined. This paper extends this discussion into a more detailed investigation of the influence of soil surface proximity on periodic water table motion.

[8] Shallow periodic water tables frequently occur in nature, in particular where aquifer systems are subject to periodic surface water forcing across a sloping boundary. One such example is the coupling of oceanic wave runup on sloping beaches where, moving toward the ocean across the beach face, the water table becomes increasingly closer to the sand surface before finally exiting the beach face forming the landward boundary of a seepage face. Because of the many complexities associated with these natural systems (for example, random periodic forcing, infiltration from wave runup and uncertainty in aquifer parameters), the present study focuses on simplified 1-D vertical sand column experiments. The findings from these experiments provide useful insights into the fundamental processes occurring in periodic flow systems which can be used to better understand natural systems.

2. Experimental Setup and Procedures

[9] The sand column shown in Figure 1 has the dimensions 1.8 m high with a 0.15 m × 0.15 m square cross-section with a 10cm deep clear water cell at its base which is connected to a variable head overflow reservoir which delivers simple harmonic forcing to the base of the sand column. The driving head (h_0) and the pore pressure at a point within the saturated zone ($h^*(z_0)$, where z_0 is an arbitrary elevation within the saturated zone) were monitored using pressure transducers. The pore pressure was monitored via a horizontal screened piezometer which extended 10 cm into the sand. The piezometer was made from 5 mm stainless steel tubes perforated with numerous 2.5 mm diameter holes screened by stainless steel mesh with 0.1 mm openings.

[10] The experimental system and sand used is the same as described in detail by *Nielsen and Perrochet* [2000], *Nielsen and Turner* [2000], and *Cartwright et al.* [2005]. The sand used was locally mined, quartz-based dune sands with a median grain diameter of d_{50} = 0.2 mm and a sorting ratio of d_{90}/d_{10} = 1.8 indicating the well-sorted nature of the sand. Sieve curves and first drying moisture retention curves of the sand can be found in the work by *Cartwright et al.* [2005]. The first moisture drying curve for this soil type was determined by *Nielsen and Perrochet* [2000] by first saturating a sample of the sand and then monitoring the decrease in moisture content as more and more suction was applied.

[11] Previous researchers [e.g., *Fayer and Hillel*, 1986; *Nachabe et al.*, 2004] have identified the significant influence of air encapsulation on the aquifer specific yield during the infiltration process. In the present experiments the sand was added to a water filled column in order to avoid air encapsu-

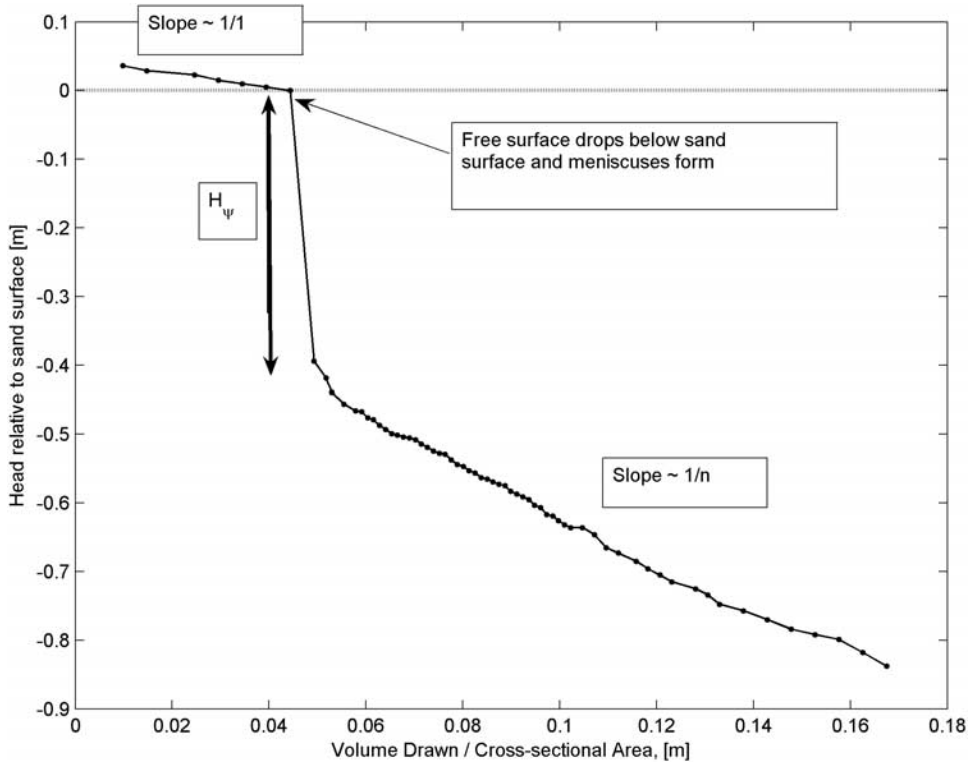

Figure 2. Pore pressure head variation with the equivalent depth of water extracted from the sand column. Note the disproportionately large pressure drop after the removal of only a minute volume water as meniscuses form at the sand surface.

lation and as the driving head is at the base of the column air encapsulation is not believed to be important in this case.

2.1 In Situ Determination of Aquifer Properties

[12] Prior to conducting the periodic flow experiments, two tests were carried out to determine various aquifers parameters in situ. First, a falling head test was performed to determine the sand column's saturated hydraulic conductivity. The column was saturated from below such that the free surface was above the sand surface and a constant head was a applied to the base of the column. The flow velocity was then observed as the rate of fall of the free surface ($w = dh/dt$) which was then equated to the Darcy flux and solved for the saturated hydraulic conductivity (K_s). Several tests were performed which yielded an average value of $K_s = 2.00 \times 10^{-4}$ m s^{-1}.

[13] The second test was conducted to determine the sand's static specific yield and the height of the capillary fringe. The sand column was first saturated such that the free surface was initially above the sand surface. Small, incremental volumes of water were extracted from the base of the column and the piezometric head in the sand was observed and recorded once it had stabilized, thus representing its new static equilibrium value. The resultant data is shown in Figure 2 where the volume extracted has been presented as the equivalent head of water extracted (volume extracted divided by the cross-sectional area of the column). The slope of the curve therefore represents the inverse of the specific yield (n) of the sand (volume of water released per unit drop in pressure head).

[14] There are three distinct parts to the curve shown in Figure 2. The first is where the free surface is above the sand surface and hence the slope of the line is approximately unity (i.e., $n = 1$). The second feature is the disproportionately large drop in pore pressure for only a small loss of water. This is a result of the free surface dropping below the sand surface and the consequent formation of meniscuses. The extent of the pressure drop is equivalent to the height of the capillary fringe which, from Figure 2, was determined to be $H_\psi \approx 0.4$ m. The third and final part of the curve has a much flatter slope as the free surface is now below the sand surface and only the pores are being drained of water. The slope of the line = $1/n \approx 1/3.49$ which yields $n \approx 0.29$.

2.2 Periodic Flow Experiments

[15] In order to examine the influence of the depth to the water table on its behavior under periodic flow conditions, all experimental parameters were held constant except for the sand surface which was lowered incrementally with each successive test. For each test the column was allowed to reach a steady periodic state before recording time series of both the driving head (h_0) and a piezometric head from within the saturated zone ($h^*(z_0 = 0.51$ m)). A steady periodic state was ensured by analyzing repeat measurements until the harmonic coefficients (amplitudes and phases) became steady. The experimental parameters are provided in Table 1 and are summarized as follows: oscillation period $T \approx 351$ s; driving head amplitude, $A \approx 0.17$ m; mean driving head level $D \approx 0.73$ m.

2.3. Data Analysis

[16] The experimental values of the complex effective porosity were derived from the present data using harmonic

Table 1. Summary of Experimental Parameters and Results[a]

z_s (m)	T (s)	D (m)	A (m)	$\|\eta\|$ (m)	ϕ (rad)	$\Re\{n_\omega\}$	$\Im\{n_\omega\}$	$\|n_\omega\|$	$-\mathrm{Arg}\{n_\omega\}$
1.40	350	0.731	0.169	0.101	0.290	0.0051	−0.0064	0.0082	0.9004
1.37	352	0.722	0.168	0.098	0.219	0.0040	−0.0073	0.0084	1.0656
1.34	351	0.708	0.167	0.100	0.296	0.0054	−0.0066	0.0085	0.8867
1.30	351	0.679	0.167	0.103	0.275	0.0051	−0.0065	0.0082	0.9049
1.27	351	0.733	0.170	0.097	0.311	0.0057	−0.0071	0.0091	0.8947
1.24	351	0.733	0.169	0.097	0.310	0.0057	−0.0070	0.0090	0.8923
1.21	351	0.731	0.170	0.103	0.314	0.0055	−0.0061	0.0082	0.8409
1.19	351	0.729	0.170	0.103	0.327	0.0057	−0.0060	0.0083	0.8155
1.17	351	0.734	0.171	0.103	0.269	0.0047	−0.0064	0.0079	0.9371
1.15	351	0.734	0.172	0.105	0.325	0.0056	−0.0059	0.0081	0.8126
1.14	351	0.734	0.170	0.104	0.300	0.0051	−0.0060	0.0079	0.8604
1.12	351	0.730	0.170	0.104	0.311	0.0054	−0.0060	0.0080	0.8383
1.08	351	0.733	0.169	0.104	0.286	0.0049	−0.0060	0.0077	0.8839
1.06	351	0.733	0.171	0.108	0.355	0.0059	−0.0052	0.0078	0.7220
1.04	351	0.732	0.172	0.107	0.309	0.0052	−0.0057	0.0077	0.8270
1.02	351	0.733	0.171	0.118	0.305	0.0046	−0.0041	0.0062	0.7208
1.00	351	0.735	0.171	0.139	0.320	0.0041	−0.0018	0.0045	0.4091
0.98	351	0.733	0.171	0.148	0.315	0.0038	−0.0011	0.0040	0.2687
0.96	351	0.723	0.169	0.145	0.320	0.0040	−0.0012	0.0041	0.2823
0.93	351	0.730	0.171	0.159	0.275	0.0031	−0.0004	0.0032	0.1195
0.90	351	0.729	0.170	0.160	0.257	0.0029	−0.0003	0.0029	0.1019
0.88	351	0.732	0.173	0.166	0.182	0.0020	−0.0003	0.0020	0.1315
0.83	351	0.729	0.170	0.148	0.242	0.0030	−0.0012	0.0032	0.3963

[a]Here z_s is the sand surface elevation; T is the oscillation period; D is the mean driving level; A and $|\eta_0|$ are the driving head and water table amplitudes; ϕ is the water table phase lag relative to the driving head; and $\Re\{n_\omega\}$, $\Im\{n_\omega\}$, $|n_\omega|$ and $-\mathrm{Arg}\{n_\omega\}$ are the real and imaginary parts, the magnitude and the (negative) argument of the complex effective porosity.

analysis and the linear frequency response approach as described in detail by *Nielsen and Perrochet* [2000] and *Cartwright et al.* [2005]. Under the assumption of a linearly responding system, the frequency response function of the water table subject to simple harmonic forcing is given by [*Nielsen and Perrochet*, 2000]

$$F(\omega) = \frac{\eta(t)}{\eta_0(t)} = |F|e^{-i\phi} = \frac{1}{1 + i\omega\frac{n_\omega D}{K_s}} \tag{3}$$

where η and η_0 are respectively the water table and driving head elevations, ϕ is the water table phase lag relative to the driving head and D is the mean driving head elevation.

[17] It follows that, in order to approach the limit of a perfectly responding system ($|F| \rightarrow 1$ and $\phi \rightarrow 0$) for a given aquifer system (fixed D and K), there must be either (1) long-period oscillations (small ω) and/or (2) small n_ω ($|n_\omega| \rightarrow 0$ and $-\mathrm{Arg}\{n_\omega\} \rightarrow 0$). It is the latter case that is relevant to the present work which focuses on oscillations with a relatively short period (T = 350 s). Referring to the definition (equation (2)) and discussion of n_ω provided in the introduction, this limiting case is therefore one in which there is limited moisture exchange occurring. This will be discussed further in relation to the present experiments in section 3.

3. Results and Discussion

3.1. Reduction in the Aquifer Storage Coefficient

[18] Figure 3 shows the influence of different sand surface elevations (and hence water table depths) on the water table response, namely, through derived values for $|n_\omega|$, $-Arg\{n_\omega\}$, $|F|$ and $-Arg\{F\}$. The approximate static-equilibrium moisture distribution, $\theta(z)$, has also been estimated using the measured first drying curve, $\theta(\psi)$, by adding the suction head, ψ, to the mean driving head elevation, D. The data are also summarized in Table 1.

[19] While the sand surface is above the region of saturated moisture ($z_s \geq D + H_\psi$) there is no measurable effect of the sand surface on the water table oscillations and the derived values of n_ω are comparable to the values derived by *Cartwright et al.* [2005]. However, once the sand surface begins to truncate the tension saturated zone of the capillary fringe ($z_s < D + H_\psi$) there is a rapid decrease in $|n_\omega|$ and $-Arg\{n_\omega\}$ until a point where the sand surface equals the maximum water table elevation ($z_s = D + |\eta|$). and the magnitude of the frequency response almost reaches unity. That is, for a limited amount of moisture exchange (i.e., small $|n_\omega|$, see sections 1 and 2.3) a disproportionately large change in pressure is observed ($|F| \rightarrow 1$). This is consistent with previous observations under steadily falling [*Childs*, 1969; *Duke*, 1972; *Nachabe*, 2002] and rising [*Fayer and Hillel*, 1986; *Nachabe et al.*, 2004] water tables that the specific yield decreases with proximity of the water table to the surface of the porous medium.

3.2. Wetting and Drying of the Sand Surface: Meniscus Formation and Deformation

[20] For $z_s < D + A$ in Figure 3, the data has limited meaning as the free surface was observed to be above the sand surface for part of the oscillation period thus voiding the governing porous media flow equation used to derive n_ω which assumes that the free surface is always below the ground surface [cf. *Nielsen and Perrochet*, 2000]. These particular experiments however reveal some interesting variations in the piezometric head observed in the saturated zone that are indicative of meniscus formation at the sand surface. Although the piezometer is not at the water table, the dynamics seen in the piezometric head below the water

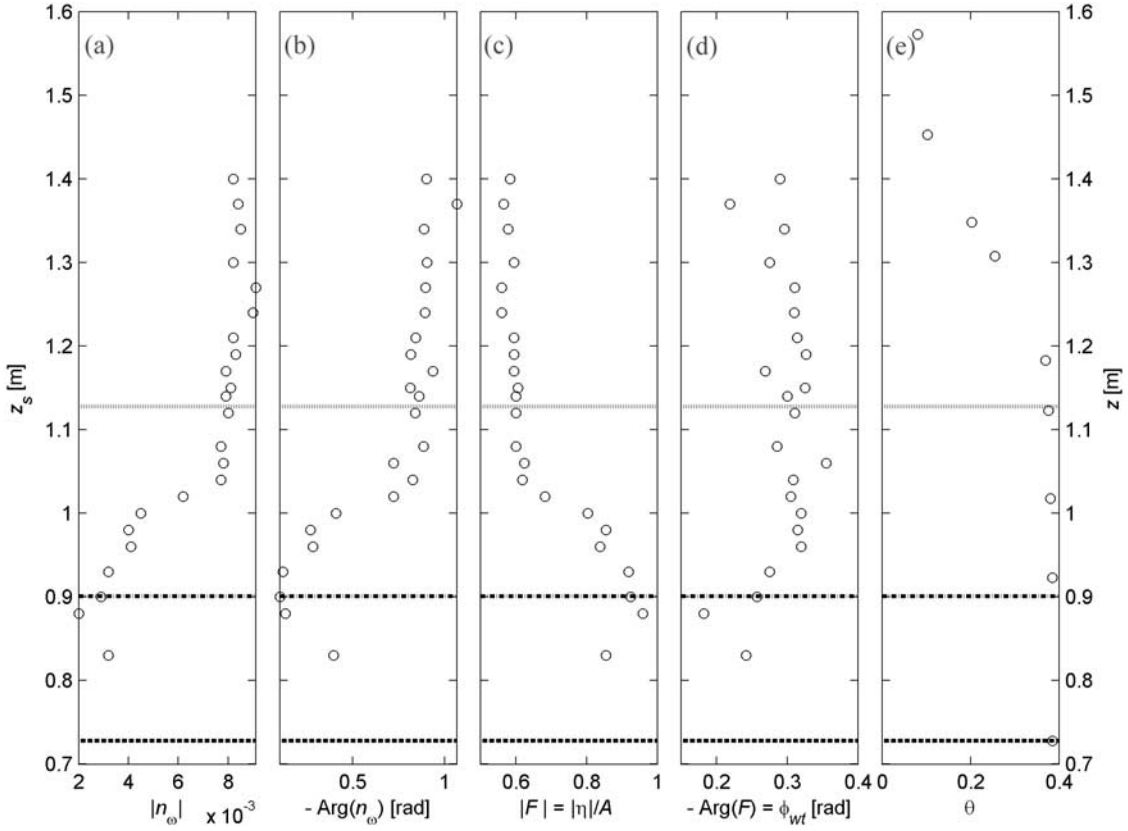

Figure 3. Influence of a truncated capillary fringe on (a) $|n_\omega|$, (b) $-Arg\{n_\omega\}$, (c) $|F|$, and (d) $-Arg\{F\}$. Also shown is (e) the equilibrium first drying curve, where $z = D + \psi$. The horizontal curves in each plot represent the mean driving head level, D (solid curve), the maximum driving head elevation, $D + A$ (dash-dotted curve), and the equivalent saturated height of the equilibrium total moisture, $D + H_\psi$ (dashed curve).

table are considered to be indicative of what would be present in the water table.

[21] A new experiment was conducted with closer attention being paid to the free surface when it transgressed the sand surface. The experimental parameters were $T = 354$ s, $D = 0.984$ m and $A = 0.167$ m with the observed time series shown in Figure 4 where the elevation of the driving head (h_0) was above the sand surface for a significant part of the oscillation period. As a consequence the free surface (h) was also observed to be above the sand surface for part of the oscillation period. This occurred between $50 < t < 200$ s where the piezometric head measured at an elevation $z_0 = 0.4$ m ($h^*(z_0, t)$) is both damped and lags the driving head.

[22] During falling water ($100 < t < 140$ s), $h^*(z_0, t)$ falls at a rate slower than the driving head level. At $t \approx 140$ s, there is a sharp drop in $h^*(z_0, t)$ which is indicative of meniscus formation at the sand surface [e.g., *Gillham*, 1984; *Nielsen et al.*, 1988]. As shown in Figure 2, meniscus formation during the falling phase only requires an amount of water of the order of 1 grain diameter ($d_{50} \approx 0.2$ mm) to be removed from the sand surface for a correspondingly large change in pressure of the order of a capillary fringe height ($H_\psi \approx 0.4$ m). This is further illustrated using the complex effective porosity definition (cf. equation (1)),

$$n_\omega = n\frac{\mathrm{d}h_{tot}}{\mathrm{d}h} \approx n\frac{d_{50}}{H_\psi} \approx n\frac{0.0002}{0.4} = 0.0005n \qquad (4)$$

That is, there is a 4 orders of magnitude reduction in the aquifer storage coefficient for this particular soil type.

[23] The piezometric head then continues to fall to a level equal to the driving head (which is less than a capillary fringe height) and then closely follows it with a slight delay during rising water ($260 < t < 360$ s). This indicates that, during this time $|F| \approx 1$ which in turn indicates that n_ω is correspondingly very small (cf. Figure 3). In a physical context, this implies that there is very little moisture exchange taking place. This, in turn, will limit the mixing of surface and sub-surface waters in natural systems such as beach groundwater systems forced by wave runup. Also, infiltration-exfiltration has been demonstrated to play a role in the mobility of sediments on beaches [e.g., *Elfrink and Baldock*, 2002] and thus in situations where the water table is significantly truncated (close to the water table exit point), and hence mass exchanged is limited, these processes will also be limited.

4. Simple "Wetting and Drying" Model

[24] The process of meniscus formation at the sand surface and its effect on the pore pressure as illustrated by the data in Figure 4 can be further supported using a simple model of the flow in the sand column derived as follows.

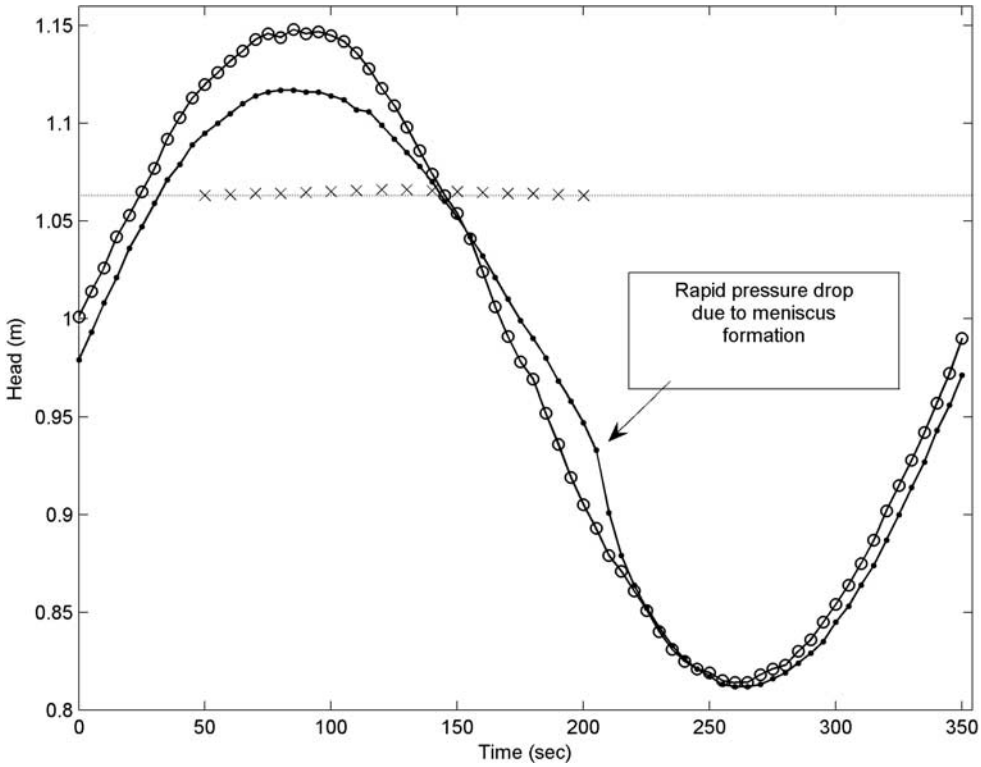

Figure 4. Observed time series from the sand column indicating the effect of meniscus formation at the sand surface. The different curves denote the driving head h_0 (solid curve with open circles), the piezometric head $h^*(z_0 = 0.4$ m) (solid curve with closed circles), the free surface observed above the sand surface (crosses), and the sand surface elevation $z_s = 1.063$ m (dotted line).

4.1. Governing Equation

[25] The dynamic flow equation for the sand column shown in Figure 1 is derived using the principle of continuity and Darcy's law which yields

$$S\frac{\mathrm{d}h_{tot}}{\mathrm{d}t} = K_s\frac{h_0(t) - h(h_{tot}, t)}{H_s(t)} \tag{5}$$

where K_s is the saturated hydraulic conductivity, S is the aquifer storage coefficient, h_0 is the driving head level, $h(h_{tot})$ is the head experienced at the level h_{tot}. The variable H_s is the equivalent saturated height of the sand column over which the head difference $h_0 - h(h_{tot})$ is acting and is defined by

$$\begin{aligned} H_s &= z_s \quad \text{if} \quad h_{tot} \geq z_s \\ H_s &= h_{tot} \,\text{if} \quad h_{tot} < z_s \end{aligned} \tag{6}$$

In adopting the equivalent saturated height of the total moisture (h_{tot}) to describe the total moisture in the column we inherently neglect the transition from complete to residual saturation above the water table. For the present application where the water table transgresses the sand surface, the water table is always within about 20 cm of the sand surface (cf. Figure 4) and therefore the 40 cm thick capillary fringe (cf. Table 2) always extends to the sand surface meaning that the column of sand remains practically saturated. Therefore very little moisture exchange is taking place and the effects of soil moisture hysteresis are negligible and hence the assumption made is considered to be sufficient to describe the system. The predictive ability of the model is discussed in section 4.3.

4.2. Incorporation of the Effects of Wetting and Drying at the Sand Surface

[26] In the solution of the governing equation (5), the cycling of the free surface across the sand surface has implications for both the storage coefficient S and the head experienced at the level h_{tot}, $h(h_{tot})$. When the free surface is at or above the sand surface ($h_{tot} \geq z_s$) then S will be equal to unity and when the free surface is below the sand surface and meniscuses have formed ($h_{tot} < z_s$), then S will be equal to the usual effective porosity n, i.e.,

$$\begin{aligned} S &= n \quad \text{when} \quad h_{tot} < z_s \\ S &= 1 \quad \text{when} \quad h_{tot} \geq z_s \end{aligned} \tag{7}$$

In order to incorporate these criteria into a numerical solution of the governing equation (5), the transition described by (7) can be mathematically represented with the following hyperbolic tangent function,

$$S(h_{tot}, t) = \frac{1+n}{2} + \frac{1-n}{2}\tanh\left(\frac{h_{tot}(t) - z_s}{L}\right) \tag{8}$$

where L is a length scale of the order of 1 grain diameter ($\approx d_{50}$) which describes how rapidly S transitions between unity and n.

[27] The head experienced at the level h_{tot}, $h(h_{tot})$, will also vary depending on whether the free surface is above or

Table 2. Summary of Simulation Parameters[a]

z_s (m)	K (m/s)	n	H_ψ (m)	d_{50} (mm)	z_0 (m)	D (m)	A (m)	T (s)
1.063	1.95×10^{-4}	0.29	0.4	0.2	0.51	0.984	0.167	354

[a]Here z_s is the sand surface elevation; D, A, and T are the mean, amplitude and period of the driving head; K is the hydraulic conductivity; n is the specific yield; H_ψ is the height of the capillary fringe; d_{50} is the grain diameter; and z_0 is the level at which the piezometric head was observed.

below the sand surface. When the free surface is at or above the sand surface then there are no meniscuses and therefore $h(h_{tot}) = h_{tot}$ and when the free surface moves below the sand surface meniscuses begin to form and $h(h_{tot})$ will be reduced from h_{tot} by an amount equal to $H_\psi \cos\varphi$, where φ is the contact angle of the fluid with the sediment and H_ψ is the equivalent saturated height of a fully developed capillary fringe. In other words, when there are no meniscuses $\varphi = 90°$ and hence $h(h_{tot}) = h_{tot}$ and when the meniscuses are fully developed then $\varphi \approx 0$ and $h(h_{tot}) = h_{tot} - H_\psi$. This transition can again be incorporated into the model using a hyperbolic tangent function,

$$h(h_{tot}, t) = h_{tot}(t) + \frac{H_\psi}{2}\left[\tanh\left(\frac{h_{tot}(t) - z_s}{L}\right) - 1\right] \qquad (9)$$

4.3. Model-Data Comparison and Discussion

[28] The governing equation (5) is solved numerically using a finite difference algorithm run over a sufficient number of periods to ensure that a steady oscillatory solution has been reached. The driving head in the model was generated using the harmonic parameters extracted from the observed driving head, namely, T = 354 s, D = 0.984 m, A = 0.167 m and phase, ε = 1.496 rad in the simple harmonic boundary condition,

$$h_0(t) = D + A\cos(\omega t - \varepsilon) \qquad (10)$$

To facilitate a direct comparison between the model results and the experimental observations of the piezometric head, an expression for $h^*(z_0, t)$ is derived as follows. In the presence of vertical flows, the piezometric head at some elevation z_0 can be derived using [*Nielsen and Perrochet*, 2000]

$$h^*(z_0, t) = h(h_{tot}, t) + \int_{z_0}^{h_{tot}} \frac{w}{K_s} dz \qquad (11)$$

where $w = K_s\,[h_0\,(t) - h(h_{tot}, t)]/h_{tot}$ is the vertical velocity which when combined with (11) leads to

$$h^*(z_0, t) = h_0(t) - \frac{h_0(t) - h(h_{tot}, t)}{h_{tot}} z_0 \qquad (12)$$

The model-data comparison is shown in Figure 5, which indicates that the model is able to predict the observed

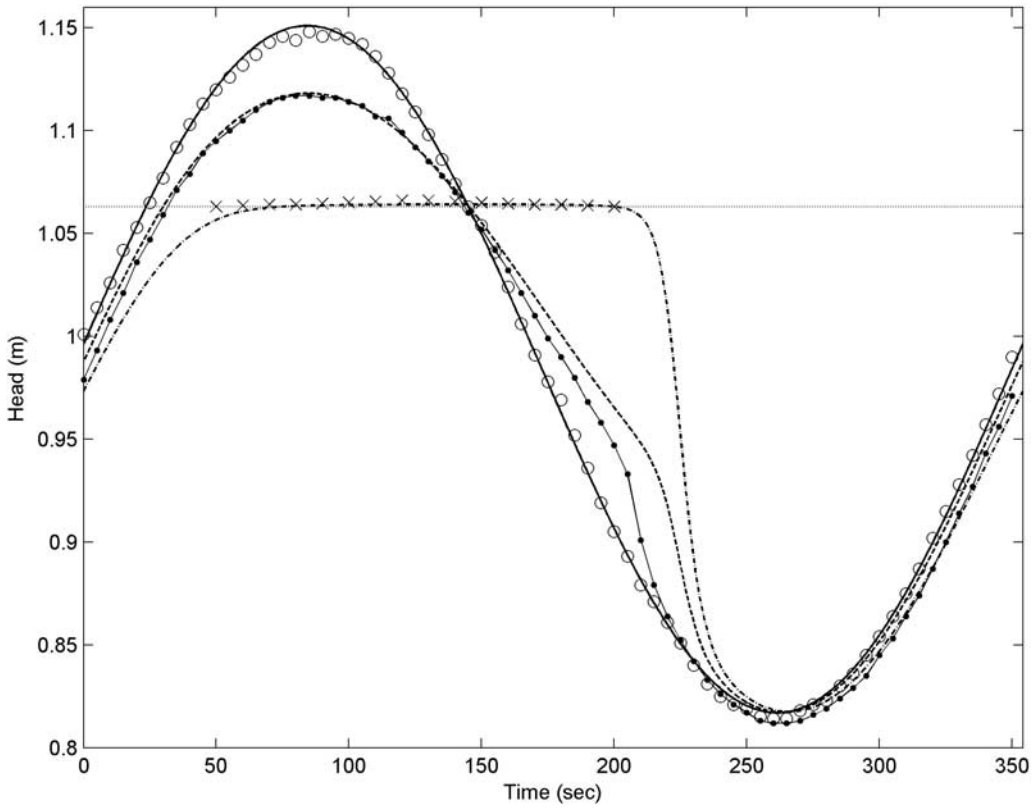

Figure 5. Comparison between the simple wetting and drying model results and experimental data. The curve and symbol types are defined for the driving head (open circles, observed; solid curve, fitted), the piezometric head $h^*(z_0 = 0.4$ m) (closed circles with solid curve, observed; dashed curve, simulated), the observed free surface (crosses), simulated $h(h_{tot})$ (dash-dotted curve), and the sand surface (dotted line).

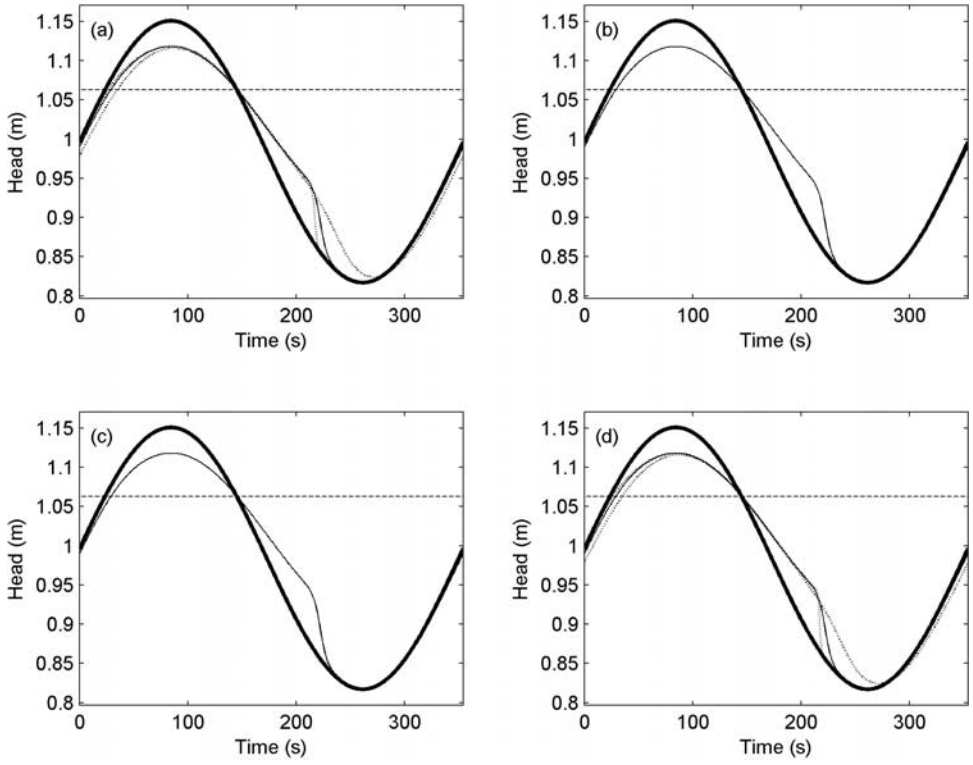

Figure 6. Sensitivity of the simple wetting and drying model to input parameters. (a) Hydraulic conductivity, $K = [5 \times 10{-}^{4}; 5 \times 10^{-5}]$ m s^{-1}. (b) Effective porosity, $n = [0.2; 0.4]$. (c) Capillary fringe height, $H_\psi = [0.3; 0.5]$ m. (d) Transition length scale, $L = [d_{50}/4; 4\ d_{50}]$. The different curve types correspond to h_0 (thick solid curve), $h^*(z_0 = 0.4$ m), using experimental parameters listed in Table 2 (thin solid curve), and $h^*(z_0 = 0.4$ m), parameter sensitivity curves (dash-dotted curve). The bold curves in each plot correspond to the results obtained using the experimental parameters listed in Table 2.

behavior, including the presence of the free surface above the sand surface for 60 s < t < 210 s. The model also performs reasonably well at the time of meniscus formation ($t \approx 220$ s), capturing the timing and extent of the rapid pressure drop, albeit with a slight overprediction of $h^*(z_0)$. The model also accurately predicts the near perfect response of the pore pressure to the driving head during the rising phase ($t > 250$ s).

4.4. Model Sensitivity

[29] Figure 6 provides an indication of the ''wetting and drying'' model's sensitivity to the various input parameters (K_s, n, H_ψ and L) which were individually varied within a realistic range of values for this soil type (see figure caption for details). In all cases the predicted h_{tot} is seen to be insensitive to the range of parameters tested under the present forcing conditions. The predicted $h^*(z_0 = 0.4$ m) is also seen to be mostly insensitive to the parameters tested with the exception of some moderate sensitivity to K_s and L (Figures 6a and 6d) in regards to the rapid pressure drop at the time of meniscus formation. That is, a larger K_s and/or smaller L lead to a faster drop in pressure and vice versa.

5. Finite Element Richards Equation Modeling

[30] The wetting and drying problem illustrated by the data in Figure 4 provides an interesting test case for the numerical solution of the Richards equation with a special feature to account for the surface boundary condition. In this instance the software FEFLOW [*Diersch*, 2007] was used with the *van Genuchten* [1980] moisture-pressure model. The model parameters are the same as used for the simple model described previously in section 4 (see Table 2) with the addition of the two *van Genuchten* parameters, $\alpha = 2.5$ 1/m and $\beta = 20$ which correspond to $H_\psi = 0.4$ m.

[31] The sand column was discretized into one array of thin, vertical 2-D finite elements with unit width and thickness of 1 mm. To mimic the periodic ponding process at the surface, and the corresponding, transient head boundary condition, a horizontal 1-D discrete element is used at the sand-air interface. In that element the saturated specific storage coefficient is defined as the inverse of the element thickness and set equal to one. Activated only under positive pressure heads (free surface above the fully saturated sand column) and deactivated otherwise, this discrete element with special unity-storage feature, combined with a classical no-flow condition at all times, ensures that any change in hydraulic head in that element exactly corresponds to a change in the free surface elevation. As soon as the free surface drops below the sand surface, negative pressures lead to the deactivation of the surface element and the process is classically governed by capillary capacity and unsaturated flow until the next fully saturated phase.

[32] Compared to other ways of implementing such a complex surface boundary condition, i.e., flux-dependent head condition while the free surface is above sand surface and no-flow condition; otherwise, the approach proposed

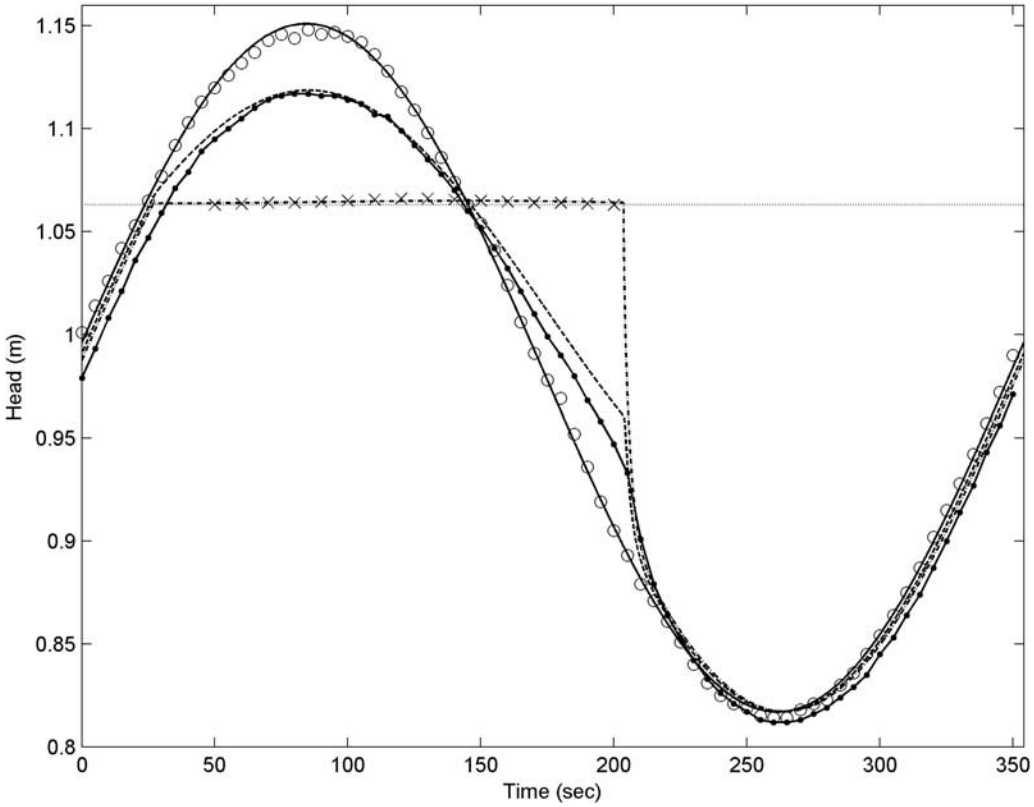

Figure 7. Comparison between the numerical Richards equation model results and experimental data. The curve and symbol types are defined for the driving head (open circles, observed; solid curve, fitted), the piezometric head $h^*(z_0 = 0.51$ m) (solid circles and curve, observed; dashed curve, simulated), the observed free surface (crosses), simulated $h(h_{tot})$ (dash-dotted curve), and the sand surface (dotted line).

here is by far the most straightforward and provides an excellent match of the observed data (cf. Figure 7).

6. Conclusions

[33] New experimental data on the behavior of a shallow periodic water table in a simplified 1-D sand column aquifer has been presented and discussed. The data show a significant reduction in the dynamic effective porosity as the capillary fringe becomes increasingly truncated. A reduction in the dynamic effective porosity (the ratio of the rate of change in total moisture to the rate of change in water table fluctuations) is indicative of a reduction in moisture exchange for a given water table fluctuation. This finding for periodic flows is in agreement with previous findings for aquifers under steadily rising and falling shallow water tables. This reduction in moisture exchange has important implications for natural systems such as beach aquifers forced by wave runup. Limited moisture exchange will limit the mixing of oceanic and aquifer water bodies and will also limit the influence of infiltration-exfiltration on sediment mobility.

[34] Experiments were also conducted to demonstrate the influence of meniscus formation and deformation at the sand surface on water table dynamics where upon the formation of meniscuses there is a rapid and disproportionate drop in pore pressure. This is a consequence of the fact that the aquifer is essentially saturated to the sand surface and the removal of a minute amount of water of the order of 1 grain size results in capillary suction forces and the establishment of a capillary fringe. Again these findings for periodic flows are in agreement with similar findings for shallow water tables subject to infiltration.

[35] These findings from the experimental data were then supported through the development of a simple two zone "wetting and drying" model. The model accounts for the transition of the storage coefficient from the usual porosity to unity and the hydraulic conductivity from its usual saturated value to a much larger "surface" water value through the use of a hyperbolic tangent function. The model is shown to be in good agreement with the data. It was also demonstrated that such processes could be very easily and accurately simulated by finite element solutions of Richards equation given the inclusion of an additional surface element with special storage properties at the sand-air interface.

Notation

α van Genuchten parameter, m^{-1}.
A driving head amplitude, m.
β van Genuchten parameter.
D mean aquifer thickness, m.
d_{50} median grain diameter, mm.
ε phase of the driving head, rad.
F frequency response function.
$|F|$ amplitude ratio between water table and driving head.

ϕ phase lag between water table and driving head, rad.
φ contact angle of the fluid with the sediment.
g acceleration due to gravity, m s^{-2}.
η water table elevation, m.
η_0 driving head elevation, m.
h water table elevation (= $D + \eta$), m.
h_c equivalent (instantaneous) saturated height of the capillary fringe, m.
h_{max} maximum water table elevation, m.
h_{tot} equivalent (instantaneous) saturated height of the total moisture, m.
h^* piezometric head, m.
h_0 driving head elevation (= $D + \eta_0$), m.
h_{tot} equivalent saturated height of total moisture, m.
H_s equivalent saturated height of the sand column, m.
H_ψ equivalent (equilibrium) saturated capillary fringe height, m.
K_s saturated hydraulic conductivity, m s^{-1}.
L transitional length scale for hyperbolic tangent functions, m.
m van Genuchten parameter.
n effective porosity (= $\theta_s - \theta_r$).
n_ω complex effective porosity.
θ local moisture content.
θ_s saturated moisture content.
θ_r residual moisture content.
S aquifer storage coefficient.
T oscillation period, s.
t time, s.
w vertical flow velocity, m s^{-1}.
ω angular frequency, rad s^{-1}.
ψ suction head, m.
z_0 piezometer elevation within the saturated zone, m.
z_s sand surface elevation, m.

[36] **Acknowledgments.** The work has been funded in part by Griffith University New Researcher grant 2095650. The authors would also like to thank *Hilberts and Troch* [2006] for their fruitful discussion of our earlier work which helped motivate the present study. We also thank the three reviewers for drawing our attention to some earlier works and providing constructive criticisms which have led to an improved manuscript.

References

Barry, D. A., S. J. Barry, and J.-Y. Parlange (1996), Capillarity correction to periodic solutions of the shallow flow approximation, in *Mixing in Estuaries and Coastal Seas*, *Coastal Estuarine Stud.*, vol. 50, edited by C. B. Pattiaratchi, pp. 496–510, AGU, Washington, D. C.

Bear, J. (1972), *Dynamics of Fluids in Porous Media*, 764 pp., Elsevier, New York.

Brooks, R. H., and A. T. Corey (1964), *Hydraulic properties of porous media*, *Hydrol. Pap. 3*, Colo. State Univ., Fort Collins, Colo.

Cartwright, N., P. Nielsen, and P. Perrochet (2005), Influence of capillarity on a simple harmonic oscillating water table: Sand column experiments and modeling, *Water Resour. Res.*, *41*, W08416, doi:10.1029/2005WR004023.

Cartwright, N., P. Nielsen, and P. Perrochet (2006), Reply to comment by A. G. J. Hilberts and P. A. Troch on "Influence of capillarity on a simple harmonic oscillating water table: Sand column experiments and modeling", *Water Resour. Res.*, *42*, W11602, doi:10.1029/2006WR005188.

Childs, E. C. (1969), *An Introduction to the Physical Basis of Soil Water Phenomena*, 493 pp., John Wiley, London.

Diersch, H. J. (2007), FEFLOW reference manual 5.3, WASY Inst. for Water Resour. Plann. and Syst. Res., Berlin.

Duke, H. R. (1972), Capillary properties of soils—Influence upon specific yield, *Trans. ASAE*, *15*, 688–691.

Elfrink, B., and T. E. Baldock (2002), Hydrodynamics and sediment transport in the swash zone: A review and perspectives, *Coastal Eng.*, *45*(3–4), 149–167, doi:10.1016/S0378-3839(02)00032-7.

Fayer, M. J., and D. Hillel (1986), Air encapsulation: I. Measurement in a field soil, *Soil Sci. Soc. Am. J.*, *50*, 568–572.

Gillham, R. W. (1984), The capillary fringe and its effect on water-table response, *J. Hydrol.*, *67*, 307–324, doi:10.1016/0022-1694(84)90248-8.

Hilberts, A. G. J., and P. A. Troch (2006), Comment on "Influence of capillarity on a simple harmonic oscillating water table: Sand column experiments and modeling" by Nick Cartwright et al., *Water Resour. Res.*, *42*, W11601, doi:10.1029/2006WR005042.

Lehmann, P., F. Stauffer, C. Hinz, O. Dury, and H. Flühler (1998), Effect of hysteresis on water flow in a sand column with a fluctuating capillary fringe, *J. Contam. Hydrol.*, *33*(1–2), 81–100, doi:10.1016/S0169-7722(98)00066-7.

Li, L., D. A. Barry, J.-Y. Parlange, and C. B. Pattiaratchi (1997), Beach water table fluctuations due to wave run-up: Capillarity effects, *Water Resour. Res.*, *33*(5), 935–945, doi:10.1029/96WR03946.

Nachabe, M. H. (2002), Analytical expressions for transient specific yield and shallow water table drainage, *Water Resour. Res.*, *38*(10), 1193, doi:10.1029/2001WR001071.

Nachabe, M. H., C. Masel, and J. Obeysekera (2004), Observations and modeling of profile soil water storage above a shallow water table, *Soil Sci. Soc. Am. J.*, *68*, 719–724.

Nielsen, P., and P. Perrochet (2000), Watertable dynamics under capillary fringes: Experiments and modelling, *Adv. Water Resour.*, *23*(1), 503–515. (Correction, *Adv. Water Resour.*, *23*, 907–908, doi:10.1016/S0309-1708(00)00024-5.)

Nielsen, P., and I. Turner (2000), Groundwater waves and water exchange in beaches, paper presented at 27th International Conference on Coastal Engineering, Am. Soc. of Civ. Eng., Sydney, N. S. W., Australia.

Nielsen, P., G. A. Davis, J. M. Winterbourne, and G. Elias (1988), Wave setup and the water table in sandy beaches, *Tech. Memo.*, 88/1, 132 pp., N. S. W. Public Works Dep., Sydney, N. S. W., Australia.

Parlange, J.-Y., and W. Brutsaert (1987), A capillarity correction for free surface flow of groundwater, *Water Resour. Res.*, *23*(5), 805–808, doi:10.1029/WR023i005p00805.

Stauffer, F., and W. Kinzelbach (2001), Cyclic hysteretic flow in porous medium column: Model, experiment, and simulations, *J. Hydrol.*, *240*(3–4), 264–275, doi:10.1016/S0022-1694(00)00382-6.

van Genuchten, M. T. (1980), A closed form equation for predicting the hydraulic conductivity of unsaturated soils, *Soil Sci. Soc. Am. J.*, *44*, 892–898.

N. Cartwright, Griffith School of Engineering, Griffith University, Southport, Qld 9726, Australia. (n.cartwright@griffith.edu.au)

P. Nielsen, Division of Civil Engineering, University of Queensland, Brisbane, Qld 4072, Australia.

P. Perrochet, Centre of Hydrogeology, University of Neuchâtel, CH-2000 Neuchâtel, Switzerland.